Photorefractivity in Nanostructured Tin-Silicate Glass Ceramics: A Radiation-Induced Nanocluster Size Effect

N. Chiodini, A. Paleari,* and G. Spinolo

Istituto Nazionale Fisica della Materia - Department of Material Science, University of Milano-Bicocca, via Cozzi 53, I-20125 Milano, Italy

(Received 18 July 2002; published 6 February 2003)

The possibility of obtaining permanent photoinduced refractive index changes, up to -10^{-3}, in nanostructured silica-based composites has been demonstrated in SiO_2:SnO_2 optical-grade glass ceramics exposed to ultraviolet radiation. Optical and electron paramagnetic resonance data suggest that the negative refractive index change involves a modification at the surface of the SnO_2 nanoclusters, leading to a reduction of their crystalline size.

DOI: 10.1103/PhysRevLett.90.055507 PACS numbers: 81.05.Pj, 42.70.Gi, 61.80.Ba, 81.07.Bc

Material science already showed in the past how new complex physical properties may arise from particular aggregation states of the matter, often achievable only by means of *ad hoc* synthesis methods. Nanostructured materials are perhaps one of the best examples, which led to the foundation of the physics of quantum-confined systems [1] and its applications in photonics. Silica-based nanostructured glass ceramics are particularly interesting in this regard, mainly as lasing systems [2] and nonlinear all-optical devices [3]. Photorefractivity, that is, the property of changing the refractive index by photoactivation, is another important feature in photonics. Indeed, the ultraviolet (UV)-induced permanent photorefractivity of silica-based glasses for fiber optics [4] is the basis for the Bragg-gratings technology of in-fiber filters and planar waveguides [5,6]. Several works were carried out to understand the physical mechanisms responsible for the UV-induced refractive index changes in silicate glasses [5,7–9]. However, no study was done on a possible glass-ceramics photorefractivity. Here we report our investigation on the UV photorefractivity we found in nanostructured silica-based glass ceramics containing SnO_2 crystallites grown from an oversaturated Sn-doped silica xerogel. Our study shows that the underlying physical mechanism is different from the photorefractive response in doped glasses, and it is strictly related to a radiation-induced change of cluster size. A similar effect is expected in other materials and it could serve as a model for the optimized processing of nanostructures.

Silica samples were prepared with 0.4 to 5 mol% SnO_2 by cogelling $Si(OCH_2CH_3)_4$ (TEOS) and $Sn(CH_2CH_2CH_2CH_3)_2(OOCCH_3)_2$ in ethanol, as a solvent, by adding H_2O (TEOS/H_2O 1:8 molar ratio, TEOS/ethanol 1:3 volume ratio). Gelation occurred in a few days at 35 °C. Xerogel was then obtained by slowly evaporating the solvent. The final transparent glass ceramics has been produced by heating in O_2 (4 °C/h) up to complete densification at 1050 °C [10].

The nanometric structure of the composite materials was analyzed by means of transmission electron microscopy (TEM): Fig. 1(a) shows the homogeneous nanostructured features, while Fig. 1(b) reports a high-resolution TEM (HRTEM) image showing the crystalline structure inside the nanoclusters. The values of separation between lattice layers correspond to lattice parameters of the rutile structure of the SnO_2 cassiterite phase.

Refractive index measurements at 980 nm were carried out by using the prism coupler technique. Samples, 1 mm thick with optically polished surfaces of about 1 cm^2, were faced on a prism mounted on a high-resolution rotary table. The refractive index n of the investigated SiO_2:SnO_2 glass ceramics depends quite linearly on the volume fraction y of SnO_2 [Fig. 2(a)]. An effective medium description of the dielectric response of the composite, supposing spherical crystalline particles with refractive index $n_c(SnO_2) = 1.99$ in a glass with $n_g(SiO_2) = 1.45$, gives the Maxwell-Garnett relation [11]:

$$\frac{n^2 - n_g^2}{n^2 + 2n_g^2} = y\frac{n_c^2 - n_g^2}{n_c^2 + 2n_g^2}. \quad (1)$$

Because of the quite limited y range, Eq. (1) can be simplified to first order in y:

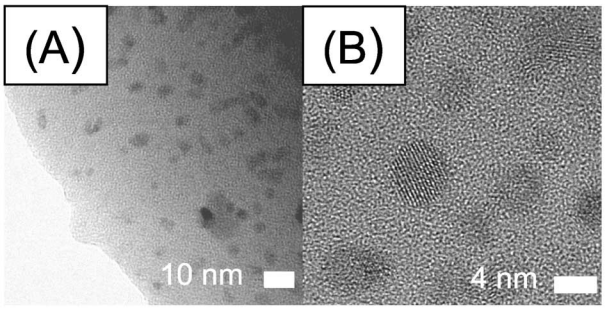

FIG. 1. (A) TEM and (B) HRTEM images of SnO_2 crystalline clusters dispersed in SiO_2 glass in 1.6 mol% SnO_2-doped silica glass ceramics prepared by the sol-gel method.

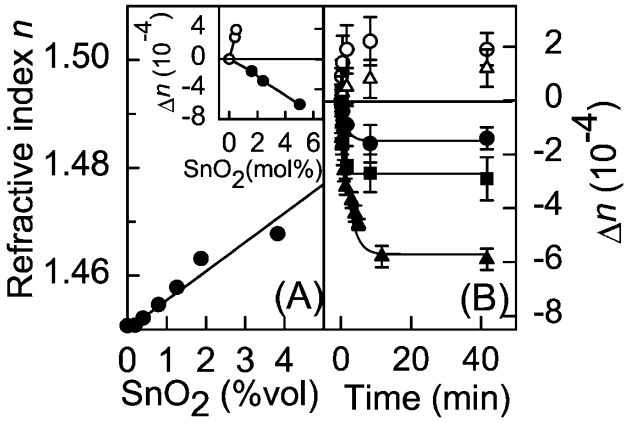

FIG. 2. (A) Refractive index of SiO_2:SnO_2 glass ceramics vs SnO_2 volume fraction; (B) refractive index change vs UV laser exposure time (at 266 nm, repetition rate 10 Hz) at a pulse energy density of 150 mJ/cm^2 in tin-silicate glass ceramics with 5 mol % SnO_2 (filled triangles), 2.4 mol % SnO_2 (filled squares), 1.6 mol % SnO_2 (filled circles), and in Sn-doped silica glass with 0.5 mol % of Sn at 170 mJ/cm^2 per pulse (open triangles) and at 340 mJ/cm^2 per pulse (open circles). Curves are obtained from Eqs. (6) and (7) (see text). Inset: saturation Δn value at 150 mJ/cm^2 per pulse vs SnO_2 mol %.

$$n \simeq n_g + y(n_c - n_g)\frac{3(n_c + n_g)}{2(n_c^2 + 2n_g^2)} \simeq n_g + y(n_c - n_g). \tag{2}$$

This relation is verified by samples with more than 0.5 mol % of SnO_2 resulting in a linear increment of refractive index of about 0.4×10^{-2} mol %$^{-1}$ of SnO_2. At lower doping levels, when no evidence of SnO_2 clustering appears in the UV absorption spectrum [10], n does not differ significantly from n_g.

The effects of exposure to intense UV beams were studied by using the fourth harmonic at 266 nm of a pulsed Nd-YAG laser (pulse duration 6 ns, repetition rate 10 Hz) at pulse fluence ranging from 60 to 340 mJ/cm^2. The thickness of the irradiated material is estimated to be about 10 μm at 266 nm from the measure of the absorption coefficient in a thin sample. Figure 2(b) shows that the UV-induced refractive index change Δn drastically depends on the presence or absence of SnO_2 nanocrystallites: when the Sn doping level is low enough to assure the dispersion of Sn atoms in substitutional Si positions in the glass, UV exposure causes an increase of n, as already observed [12]. By contrast, SiO_2:SnO_2 glass ceramics show negative Δn [Fig. 2(b)]. The kinetics of Δn vs exposure time follows a saturation behavior, with a saturation value quite linearly dependent on the UV power density. At fixed laser exposure conditions, Δn is approximately proportional to the molar SnO_2 concentration (inset in Fig. 2), with a change of -1.2×10^{-4} for each mol % of SnO_2 after 10^4 pulses at 150 mJ/cm^2 per pulse. Indeed, the achievable Δn is not limited by the solubility of tin in silica [10], and negative Δn of 10^{-3} can be obtained.

Figure 3(a) shows the results of isochronal annealing experiments of 30 min from 100 to 900 °C. The starting refractive index was approximately restored after 30 min at 700 °C. However, reirradiation after treatment at 700 °C did not induce the same Δn value observed after the first irradiation, resulting in a decrease of the photosensitivity. This memory effect was further investigated by means of repeated irradiation-annealing cycles. We found a lower irradiation effect after each annealing at 700 °C [inset in Fig. 3(a)]. By contrast, annealing treatments at 900 °C removed memory effects.

The response of the material to repeated irradiation-annealing cycles was also investigated by electron paramagnetic resonance (EPR), looking for UV-induced paramagnetic species [Fig. 3(b)]. After the first irradiation, a signal at $g = 2.001$ was observed, suggesting the formation of Si-E' centers, i.e., unpaired sp^3-like electrons in threefold coordinated Si sites in the tetrahedral-coordinated silica network [13]. No evidence of Sn-E' centers (the Sn variants of E' centers [14]) was observed [curve a in Fig. 3(b)]. This result indicates that the silica host is quite Sn free, all tin atoms being clustered in the crystalline oxide nanophase where the formation of E'-like defects is not compatible with the SnO_2 octahedral-coordinated network. Nevertheless, irradiation after annealing at 700 °C gave rise to a measurable Sn-E' signal, identified through the high field structure at 341 mT due to the orthogonal component of the g tensor

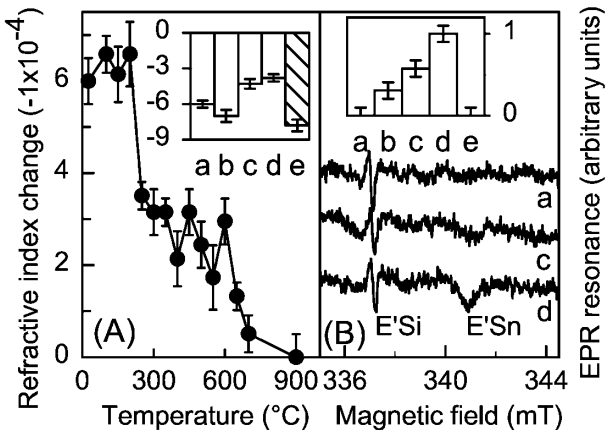

FIG. 3. (A) Effects of isochronal annealing treatment of 30 min on the UV-induced Δn in tin-silicate glass ceramics with 5 mol % SnO_2. Inset: evolution of the UV-induced (pulse energy density 150 mJ/cm^2) Δn from the starting value (a) through repeated cycles (a)–(d) of annealing treatments (30 min at 700 °C) and UV irradiation, and (e) after an annealing at 900 °C for 30 min followed by a final reirradiation at the same conditions. (B) UV-induced EPR spectra (and relative signal amplitude of the Sn-E' resonance at 341 mT, in the inset) during the same annealing-irradiation cycles.

[14] [curves *c* and *d* in Fig. 3(b)]. Its intensity slightly grew after repeated irradiation-annealing cycles [inset in Fig. 3(b)], similarly to the decrease of photosensitivity.

The combined analysis of EPR and Δn data as a function of irradiation-annealing cycles gives a valuable indication of the involved processes. The observation of a Sn-E' signal indicates that a thermal treatment after UV irradiation can disperse a fraction of the Sn content from the nanophase to the glass matrix: this process furnishes Sn sites acting as precursors of UV-induced formation of Sn-E' centers. Nevertheless, a thermal treatment alone, without a previous UV irradiation, cannot disperse Sn atoms from the crystalline SnO_2 clusters: the cluster formation itself is a thermally activated process [10]. Therefore, the thermal diffusion of Sn atoms resulting from EPR data cannot proceed from the crystalline nanoclusters, but from a distinct radiation-induced phase, probably formed at the crystallite-glass boundary as a result of the strong energy release during the UV irradiation (see Fig. 4). Indeed, at 266 nm (4.66 eV), the glassy matrix of the material is substantially transparent to the radiation that is instead strongly absorbed by the SnO_2 nanophase because its energy is above the onset of band-to-band transitions at 3.6–4 eV. Data in Fig. 3(b) also indicate that the source of thermally diffusing Sn, as well as Sn atoms already diffused into the glass, are removed from the glass by annealing at 900 °C, and the starting refractive index and photosensitivity are restored. This can be interpreted as a reclustering of Sn in crystalline SnO_2, with a consequent reestablishment of the starting conditions. At 700 °C, only a partial recovery of the pristine cluster sizes occurs, accompanied by Sn diffusion from the external surface of the UV-induced phase towards the glass (causing the formation of Sn-E' precursors, increasing the glass index, and giving to the glass the positive photorefractivity of Sn-doped silica [12]).

Based on these data, one can argue that UV irradiation causes a reduction, from y_0 to y_∞, of the volume fraction occupied by the crystalline SnO_2 nanophase. Bond-breaking and Sn diffusion may indeed give rise to a local rearrangement, causing the transformation of the interface layers in an amorphous mixed phase. The resulting cluster-size reduction is supported by independent spectroscopic evidence we obtained from low temperature photoluminescence excitation (PLE) spectra [Fig. 5(a)]. The structure at 4 eV, shifting towards high energy after UV irradiation, is ascribable to excitons in SnO_2 clusters in a strong quantum confinement regime [15]. The cluster-size dependence of the exciton peak position E_{exc} and the relation between the shift ΔE due to a reduction of the cluster size r_0 and the size change Δr are [1]

$$E = E_{\text{exc}} - E_G \sim \frac{1}{r^2}, \qquad \frac{\Delta E}{E} = -2\frac{\Delta r}{r_0}. \tag{3}$$

The energy shift gives a cluster-size decrease of about 5%. This means that $(y_0 - y_\infty)/y_0$ should be about 14%.

The reduction of the mean crystallite size, down to an asymptotic r_∞ value, may be described by a nonlinear system of differential equations:

$$\begin{cases} \frac{dr}{dt} = -kr^2, \\ \frac{dk}{dt} = -h(r - r_\infty), \end{cases} \tag{4}$$

where the first equation accounts for the dependence of the cluster-size reduction upon the interface area, which is the active region during the process. The second equation describes how the transformed cluster shell can induce the decrease of the rate k of transformation of inner layers, for instance, by impeding Sn diffusion towards the glass. An analytic solution may be found linearizing the system around the equilibrium point $r = r_\infty$, $k = 0$:

$$r(t) = (r_0 - r_\infty)e^{-h^{1/2}r_\infty t} + r_\infty, \tag{5}$$

$$y(t) = \sum_{m=0}^{3} a_m(r_0, r_\infty)e^{-mh^{1/2}r_\infty t}. \tag{6}$$

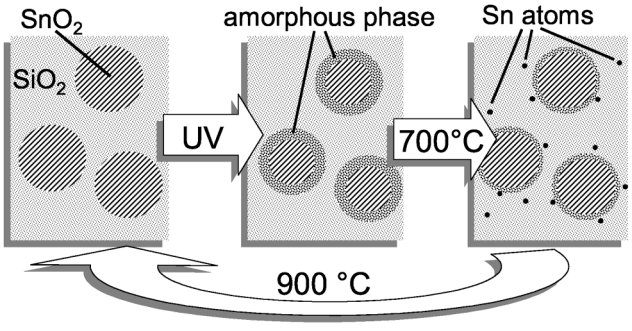

FIG. 4. Schematics of the proposed model of glass-ceramics photorefractivity based on nanocluster effects.

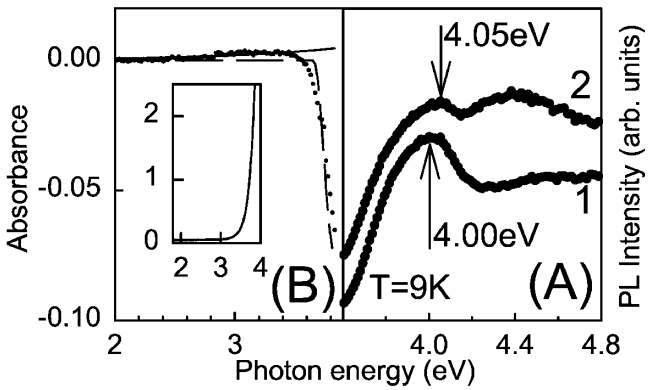

FIG. 5. (A) PL excitation spectra at 9 K (emission at 2.4 eV) of 5 mol % SnO_2-doped silica glass ceramics before (curve 1) and after (curve 2) UV irradiation (pulse energy density 150 mJ/cm^2); (B) UV-induced change of optical absorption spectra [solid and dashed curves are from Eqs. (8) and (9), respectively]. Inset: absorption spectrum before irradiation.

Based on $y(t)$, we can write the time evolution of $\Delta n(t)$ within the same approximation of Eq. (2):

$$\Delta n(t) = [n_c - n_a][y(t) - y_0], \tag{7}$$

where n_a is the index of the transformed phase. Equation (7) allows us to estimate n_a through the $(y_0 - y_\infty)$ value we independently obtained from PLE data: taking a SnO_2 concentration of 5 mol% and an experimental $\Delta n \simeq -6 \times 10^{-4}$, we calculate $n_a = 1.89 \pm 0.01$. This value supports the formation of a Sn-rich amorphous tin-silicate. Moreover, we may use $\Delta r/r_0$ from PLE data, together with r_0 from TEM analysis [15], as input data for fitting $\Delta n(t)$ through Eqs. (6) and (7). Incidentally, we note that the relatively small $\Delta r/r_0$ value justifies the approximation behind the linearization of the system (4). The model, quite sensitive to r_0, succeeds [see curves in Fig. 2(b)] in reproducing data on samples with different SnO_2 content (from 1.6 to 5 mol%) and different mean cluster size ($2r_0$ from 3 to 9 nm) with nearly the same set of parameter values. Specifically, the analysis gives $h^{1/2} = 0.0035 \pm 0.0005\ \mathrm{nm}^{-1}\,\mathrm{s}^{-1}$ and $n_a = 1.91 \pm 0.01$, the latter value in good agreement with the PLE analysis.

Further details on the cluster-size-based photorefractivity can be obtained from the UV-induced optical absorption changes [Fig. 5(b)]: an absorption increase below 3.5 eV is accompanied by a decrease at higher energy. The optical absorption in this region [inset in Fig. 5(b)] is determined by two main contributions. Electronic excitations inside the nanocrystallites give rise to a discrete spectrum whose components are significantly broadened by a distribution of E values due to cluster-size dispersion. As a result, one band [similar to that in Fig. 5(a)] is often observed in quantum-dot systems [3], superimposed on a smooth absorption spectrum whose intensity increases at high energy. The low energy tail of this contribution can be approximately described by [16]

$$\alpha_s(h\nu) \sim \exp\left[-\frac{r^2}{2\sigma_r^2}\left\{1 - \left(\frac{E_{\mathrm{exc}}(r)}{h\nu}\right)^{1/2}\right\}^2\right], \tag{8}$$

where σ_r is the variance of the cluster-size distribution. Another contribution comes from the disorder-related distribution (with variance σ_d) of localized levels due to the UV-induced interphase, giving an absorption tail we may describe, not too close to E_G, as [17]

$$\alpha_d(h\nu) \sim \exp[(h\nu - C)/\sigma_d]. \tag{9}$$

A cluster-size-based model of photorefractivity implies a change of both α_s and α_d, because of the decrease of the mean cluster size and the formation of an amorphous interphase. This model is consistent with the data, which can be reproduced qualitatively by Eqs. (8) and (9) [curves in Fig. 5(b)] from r_0, Δr, E_{exc}, and ΔE.

An estimation of the influence of the absorption changes on Δn through the Kramers-Kronig (K-K) relations shows that the intensity decrease above 3.5 eV largely overcomes the small increase in the visible spectrum. Extending the K-K integration up to 3.7 eV (above 3.7 eV the transmitted signal falls below the instrument sensitivity) and taking into account the thickness of the irradiated volume, we find $\Delta n \simeq -10^{-5}$. Nevertheless, from 3.7 to 4.1 eV, the absorption coefficient increases at least by a factor of 10, as suggested by PLE [Fig. 5(a)] with a resulting Δn of the order of -10^{-4}. In spite of the severe limitations deriving from the restricted K-K integration range, this estimation suggests that the cluster-size effect on the SnO_2 absorption contributes significantly to the glass-ceramics photorefractivity.

In summary, we have obtained a nanostructured silica-based glass-ceramic composite where a crystalline nanophase behaves as a reservoir of high refractive index material that can be suitably reduced or restored by controlled irradiation and thermal treatments. More generally, such a process could also give a method for modifying a composite on a nanometer scale.

This work is part of a National Project partially supported by the Italian Government.

*Electronic address:alberto.paleari@mater.unimib.it

[1] U. Woggon, *Optical Properties of Semiconductor Quantum Dots* (Springer-Verlag, Berlin, 1997), Chap. 2.
[2] V. I. Klimov *et al.*, Science **290**, 314 (2000).
[3] N. Peyghambarian *et al.*, in *Nanomaterials, Synthesis, Properties and Applications*, edited by A. S. Edelstein and R. C. Cammarata (Institute of Physics Publishing, Bristol, 1996), Chap. 16.
[4] P. Niay *et al.*, Opt. Mater. **11**, 115 (1999).
[5] B. Poumellec and F. Kherbouche, J. Phys. III (France) **6**, 1595 (1996).
[6] B. G. Potter, Jr. and K. Simmons-Potter, Nucl. Instrum. Methods Phys. Res., Sect. B **166–167**, 771 (2000).
[7] J. Canning, Adv. Mater. **13**, 970 (2001).
[8] M. Kristensen, Phys. Rev. B **64**, 144201 (2001).
[9] H. G. Limberger, P. Y. Fonjallaz, R. P. Salanthé, and F. Cochet, Appl. Phys. Lett. **68**, 3069 (1996).
[10] N. Chiodini *et al.*, J. Mater. Chem. **11**, 926 (2001).
[11] J. C. Maxwell-Garnett, Philos. Trans. R. Soc. London Ser. A **203**, 385 (1904).
[12] N. Chiodini, S. Ghidini, and A. Paleari, Phys. Rev. B **64**, 073102 (2001).
[13] D. L. Griscom, J. Ceram. Soc. Jpn. **99**, 899 (1991).
[14] N. Chiodini *et al.*, Phys. Rev. B **58**, 9615 (1998).
[15] N. Chiodini, A. Paleari, D. DiMartino, and G. Spinolo, Appl. Phys. Lett. **81**, 1702 (2002).
[16] V. Ranjan, V. A. Singh, and G. C. John, Phys. Rev. B **58**, 1158 (1998).
[17] N. E. Cusack, *The Physics of Structurally Disordered Matter* (Hilger, London, 1987), Chap. 11.